IEEE Access
Multidisciplinary | Rapid Review | Open Access Journal

Received June 13, 2020, accepted June 29, 2020, date of publication July 2, 2020, date of current version July 16, 2020.

Digital Object Identifier 10.1109/ACCESS.2020.3006740

High Performance Tunable Dual-Wavelength Erbium-Doped Fiber Laser Implemented by Using Tapered Triple-Core Photonic Crystal Fiber

ZIJUAN TANG[1], ZHENGGANG LIAN[2], TREVOR M. BENSON[3], (Senior Member, IEEE), XIN WANG[1], WAN ZHANG[1], SHIBO YAN[1], AND SHUQIN LOU[1], (Member, IEEE)

[1]School of Electronic and Information Engineering, Beijing Jiaotong University, Beijing 100044, China
[2]Yangtze Optical Electronics Company Ltd., Wuhan 430205, China
[3]George Green Institute for Electromagnetics Research, University of Nottingham, Nottingham NG7 2RD, U.K.

Corresponding author: Shuqin Lou (shqlou@bjtu.edu.cn)

This work was supported in part by the National Natural Science Foundation of China under Grant 61775014.

ABSTRACT Based on tapered Triple-Core Photonic Crystal Fiber (TCPCF), a high performance tunable Dual-Wavelength Erbium-Doped Fiber Laser (DW-EDFL) is proposed and experimentally demonstrated. The mode-coupling among three cores of TCPCF appears periodically and becomes further enhanced in tapered TCPCF, which are beneficial to form a filter to select lasing wavelength. A series of tapered TCPCFs with different taper lengths are fabricated and inserted into tunable DW-EDFL as filters. Multiple groups of tunable dual-wavelength lasing outputs are achieved by using the tapered TCPCF filter with a waist diameter of 126 μm. The maximum tunable range can reach up to 14.36 nm and the side mode suppression ratio of all lasing outputs are above 52 dB. In addition, the tunable single- and triple-wavelength lasers are also obtained. The tunable single-wavelength laser has an excellent linear response to strain and can be applied to realize a high-sensitivity strain sensor with the highest strain sensitivity of -13.1 pm/$\mu\varepsilon$.

INDEX TERMS Optical fiber communication, dual-wavelength tunable fiber laser, mode coupling analysis, tapered multicore fiber.

I. INTRODUCTION

A. BACKGROUND

Dual-wavelength erbium-doped fiber laser (DW-EDFL) plays an important role in the fields of microwave generation [1], high-resolution spectroscopy [2], remote sensing [3], etc. due to their high side mode suppression ratio (SMSR), narrow line width, flexible structural design, and high robustness. The main obstacle to achieve stable dual-wavelength lasing output is the strong mode competition existed in the laser cavity because of the uniform gain broadening mechanism of erbium-doped fiber (EDF). To overcome this problem, various methods have been proposed such as cooling EDF at 77 K by liquid nitrogen [4], adopting a hybrid gain medium [5], [6], utilizing Brillouin-comb assisted four-wave mixing (FWM) [7], inducing nonlinear polarization rotation (NPR) technique in laser cavity [8], [9], introducing nonlinear optical loop mirror (NOLM) [10], constructing fiber filters based on high-birefringence FBG [11], microfiber coupler [12], multicore fiber (MCF) couplers [10], Sganac interferometer [13], multi-stage lyot filter [14], Fabry–Perot and Mach–Zehnder interferometer (MZI) [15]. MCF coupler taking advantage of the unique mode-coupling property, can produce a periodically coupled transmission spectrum and thus become a popular candidate for achieving stable and multiple dual-wavelength lasers. Yin. *et al.* reported a tunable DW-EDFL by adopting twin-core fiber (TCF) and achieved tunable bandwidth of 1.2 nm with the SMSR higher than 40 dB [16]. A four-wavelength switchable fiber laser based on twin-core EDF is achieved by Lian with a wavelength spacing of 1.1 nm and the SMSR higher than 43 dB [17]. By utilizing seven-core fiber (SCF) as a filter, He. *et al.* proposed a switchable DW-EDFL with five kinds of wavelength intervals, but the highest SMSR lower than 30 dB [18]. Zhang.*et al.* reported a single- and dual-wavelength tunable DW-EDFL by combing SCF with MZI in which the tunable range are ∼11 nm and 7 nm with the SMSR higher than 45 dB [19].

The associate editor coordinating the review of this manuscript and approving it for publication was Rentao Gu.

The taper fiber technology was reported as early as 2003 [20], and it has been proven to have strong evanescent field and mode confinement. The use of such tapered fiber as filter can achieve transmission spectrum with high extinction ratio (ER) and good comb characteristics. Thus it has been widely used in dual-wavelength lasers [21], [22]. Tong. *et al.* proposed a tunable DW-EDFL using an in-line tapered fiber filter with the tuning range of dual-wavelength lasers of 10 nm and the SMSR of each laser over 43 dB [23]. A tunable C- and L-band DW-EDFL was proposed by Zhou *et al.* using a tapered large core fiber with the tunable range of 6nm and the SMSR of 50 dB [24]. It can be concluded that taper technology can be useful for improving laser output performance significantly.

Recently, photonic crystal fiber (PCF), in which the guiding core is formed by omitting a hole at the period array of air holes, has attracted great attention because of its extremely high degree of freedom in structural design. It is generally fabricated via stacking and drawing technique, which makes the realization of a multicore PCF (MCPCF) readily [25], [26]. Compared with traditional MCF, MCPCF can easily achieve small core-to-core pitch and custom number of cores by rationally designing the size, number and location of holes [27], [28]. Besides, properly designed MCPCF can provide large mode area, low bending loss and high nonlinearity [29], [30]. Thus, filters based on MCPCF are widely studied to achieve high performance DW-EDFL. A switchable and stable DW-EDFL based on a twin-core PCF filter was constructed with the SMSR of ∼40 dB [31]. A stable and tunable DW-EDFL was demonstrated by using a twin-core PCF filter, in which the SMSR was improved to 45 dB with a fixed wavelength interval [32]. Previous reports showed that broad tunable range, flexible dual-wavelength interval and high SMSR are crucial factors of DW-EDFL in realizing tunable microwave, wide-range terahertz wave [1, 33]. However, there are few works can achieve multiple sets of tunable and stable dual-wavelength lasing output with broad tunable range and high SMSR simultaneously.

B. MOTIVATIONS AND CONTRIBUTIONS

In this paper, multiple sets of dual-wavelength tunable EDFL by using tapered triple-core photonic crystal fibers (TCPCF) based filter was investigated. Compared with previous works, there are two main differences that are stressed as follows. Firstly, the mode coupling characteristics based on the tapered MCF are analyzed and used to construct filters to select lasing wavelengths. Secondly, the effect of different waist diameters on the tunable performance of lasing output based on tapered MCF filter is theoretically studied and experimentally verified.

The following are the main contributions of this paper: (1) By analyzing the effect of different taper diameters on the mode coupling of a TCPCF filter, we obtained its effect on the tunable range of a multi-wavelength laser based on such TCPCF filter. A series of experiments have been conducted, which are consistent with the simulation results. (2) Multiple sets of tunable dual-wavelength lasing outputs with different wavelength intervals are implemented by using tapered TCPCF filters. Among them, the maximum tunable range can reach up to 14.36 nm with the SMSR of higher than 52 dB. (3) The laser can also realize tunable single- and triple-wavelength lasing outputs. The tunable single-wavelength lasing has good linearity with applied strain and can be used to realize a highly sensitive strain sensor with the sensitivity of -13.1 pm/$\mu\varepsilon$.

II. THEORETICAL ANALYSIS

A. FABRICATION OF THE TAPERED TCPCF FILTER

The tapered TCPCF filter as shown in Fig.1(a) is fabricated via fusion splicing a 2.5 cm long TCPCF between two segments of single-mode fiber(SMF); then tapering the middle region of TCPCF down to the designed diameter. The homemade TCPCF was fabricated based on the Heraeus F300 silica glass tube, which can be drawn consistently with the length of several kilometers. The cross-section image of TCPCF is shown in Fig.1(b). Three cores are arranged in an equilateral triangle with a core diameter of 5.8 μm and a core distance of 8.5μm. Air holes are periodically arranged in a triangular array with a hole diameter of 4 μm and the pitch between two adjacent holes of 4.9 μm. The fiber has an outer diameter of 144 $\pm$ 0.5 μm.

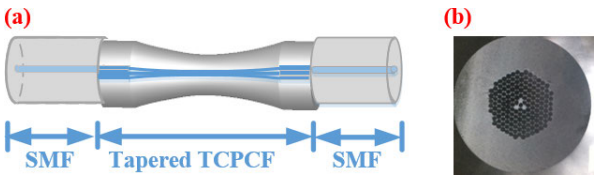

FIGURE 1. The schematic diagram of the tapered TCPCF filter (a) and the cross-section of the homemade TCPCF (b).

A commercial splicer (Fujikura, FSM-100M) is used to splice one end of TCPCF with SMF using the core-to-core splice mode built in the machine. At the other end of TCPCF, we use the splice method depicted in [16] to monitor the output power in real-time. When it gets maximum, the lead-in and lead-out SMFs are aligned to the same core of TCPCF. Then a manual splice mode is used to splice this end of TCPCF with lead-out SMF. To minimize the collapse of air holes during splicing, we optimize the fusion parameters. The degree of collapse can be evaluated by tracking the changes of output power and the glitches in the transmission spectrum because the collapse of air holes will excite multiple cladding modes, resulting in a reduction of output power and an increase of glitches in the spectrum [34]. The results show that the smallest collapse of air holes can be obtained with the arc power of -60 bit and the fusion time is 400 ms. The transmission spectrum has a small number of glitches and minimum power loss (∼5dB) with this set of splice parameters.

The fiber taper machine (Shanghai Ou Bo Optoelectronics Technology Co., Ltd.: OB-612 type) can realize two kinds

of tapering modes, i.e. flame head scan mode and non-scan mode. The amplitude of flame-scan, the width of flame head and the pulling speed are set to half of the taper length, 5 mm and 2000 μm/s, respectively. Due to the use of a fast tapering speed and relatively low temperature approach, the size of the waist area is proportionally reduced and the ratio of hole diameter to hole pitch keeps nearly constant [34]. The taper waist measured after tapering is relatively flat under the flame-scan mode and the waist diameter for 1000 μm and 2000 μm long tapers are 136 μm and 130 μm, as shown in Fig.2 (a-b). Under the non-scan mode, the taper waist has a parabolic shape with a smaller waist diameter of 126 μm and 121 μm compared with the flame-scan mode at the same taper length, as shown in Fig.2 (c-d).

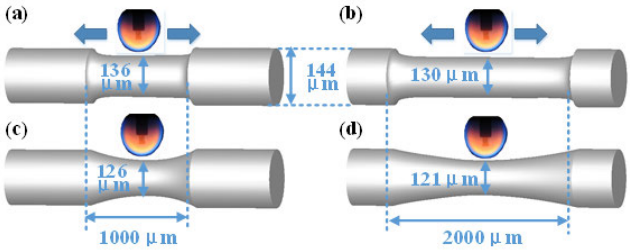

FIGURE 2. Four tapered TCPCFs with the waist diameter of 136 μm (a), 130 μm (b), 126 μm (c), 121 μm (d) under different taper mode.

B. MODE-COUPLING MECHANISM IN THE TAPERED TCPCF FILTER

This homemade TCPCF mainly supports three fundamental super-modes, each of which has two orthogonal linear polarizations. The mode profiles of three fundamental super-modes are calculated by a full vector finite-element method, as shown in Fig.3. Super-modes have different propagation constants just like modes in standard multimode fibers. Interference would appear between the super-modes with the same polarization state and thus results in the light power coupling among three cores [31]. According to mode-coupling theory, the coupling among three cores results in a periodic transmission spectrum and satisfy the following coupled-mode equation,

$$\frac{d}{dz}\begin{bmatrix} e_1 \\ e_2 \\ e_3 \end{bmatrix} = -j\begin{bmatrix} \beta_0 & c & c \\ c & \beta_0 & c \\ c & c & \beta_0 \end{bmatrix}\begin{bmatrix} e_1 \\ e_2 \\ e_3 \end{bmatrix} \tag{1}$$

where e_i is the amplitude of the electrical field of the i-th core, β_0 is the propagation constant of the mode in the isolated core, C is the coupling coefficient, which can be calculated by using the method mentioned in Ref. [35] Assuming that light is injected into the q-th core at $z = 0$ and the output power of the i-th core, $P_i(z)$ is expressed as

$$P_i(z) = e_i(z) \cdot e_i^*(z) = \begin{cases} \frac{2}{9} - \frac{2}{9}\cos(3Cz), & i \neq q \\ \frac{5}{9} + \frac{4}{9}\cos(3Cz), & i = q \end{cases} \tag{2}$$

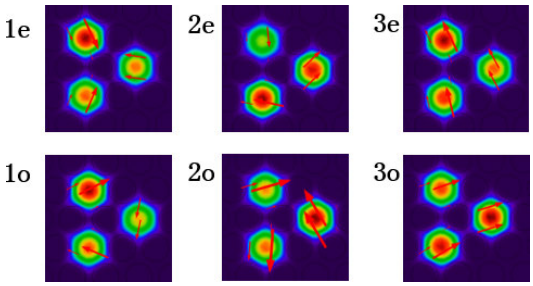

FIGURE 3. The mode profiles of three fundamental super-modes at the wavelength of 1550 nm, in which the number representing the mode order and the letter ("e" or "o") represent the two polarizations. The arrows indicate the directions of the electric fields.

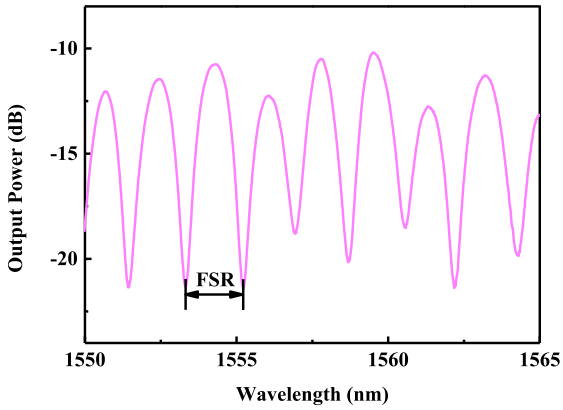

FIGURE 4. The periodic transmission spectrum of the filter before tapering.

It is known that the coupling coefficient varies linearly with wavelength. Thus, a periodic transmission spectrum can be obtained, as shown in Fig.4. The power dips in the transmission spectrum appear when the phase condition satisfies $3Cz = (2m + 1)\pi$ (m is an integer) and the corresponding wavelength is

$$\lambda_m = \frac{(2m+1)\,\pi}{3 \cdot \frac{\partial C(\lambda)}{\partial \lambda} \cdot z} \tag{3}$$

The ratio of the coupling coefficient to wavelength $\frac{\partial C(\lambda)}{\partial \lambda}$ is a constant (K) [36]. Thus the period of the transmission spectrum, which is defined as the Free Spectral Range (FSR), can be calculated by

$$FSR = \frac{2\pi}{3z \cdot K} \tag{4}$$

To investigate the effect caused by taper on coupling spectrum, the varying of coupling coefficients as a function of wavelength for tapered TCPCFs with different waist diameters are shown in Fig.5. As waist diameter increases, the coupling coefficient at the longer wavelength increases more significantly than the shorter wavelength. The high coupling coefficient is a result of the enhanced mode coupling, indicating that the output power of coupling spectrum further improved at long wavelength region. On the other hand, the slope shown in the table in Fig.5 is the ratio (K) and it

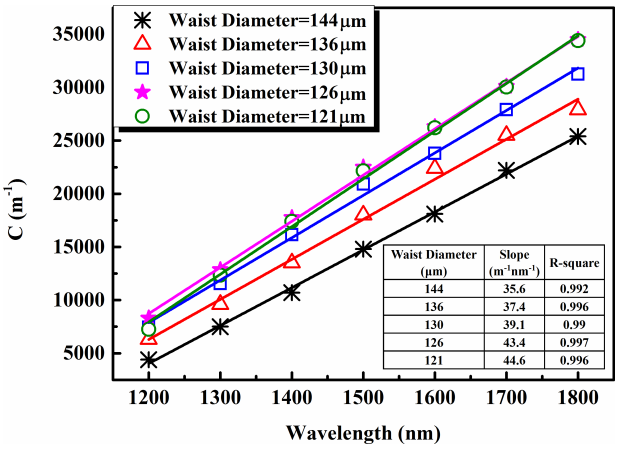

FIGURE 5. Linear fit of coupling coefficient versus wavelength under different waist diameters.

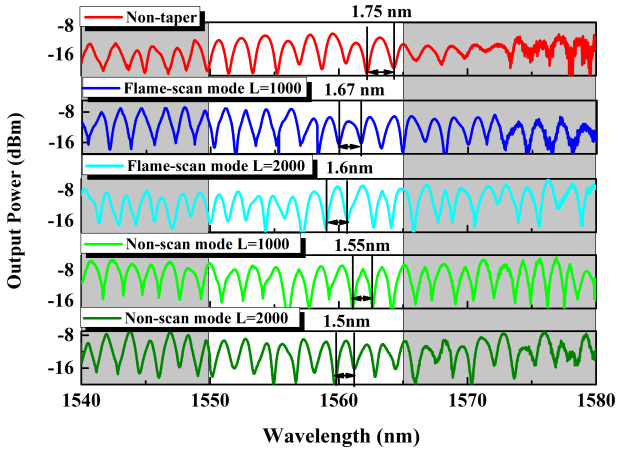

FIGURE 6. The transmission spectrum of the four tapered TCPCF filters with different tapered mode.

increases as the taper waist decreasing. According to Equations (2), the dip-wavelength (λ_m) shifts towards shorter wavelength direction as the ratio (K) increases. While the transmission spectrum drifts towards the shorter wavelength direction, the coupling in the long wavelength region is further enhanced. This indicates the transmission spectrum after tapering has some extension in both directions compared with the transmission spectrum of un-tapered TCPCF. The taper with a waist diameter of 126 μm has the highest coupling coefficient at a fixed wavelength.

When an axial strain is applied to the tapered TCPCF filter, the dip in the transmission spectrum will shift in terms of the following equation.

$$\Delta\lambda_m = -\lambda_m \cdot \varepsilon \cdot [W + 1] \tag{5}$$

Here, $\Delta\lambda_m$ is wavelength shift, ε is unit strain that can be calculated by using the moving step length of strain device (every 10 μm) divided by the distance between the two fixed ends of the tapered TCPCF filter (l) and W is a positive structure factor determined by the fiber structure. It is obvious that the dip in the transmission spectrum will shift towards the shorter wavelength with the applied strain.

C. TRANSMISSION SPECTRUM OF THE TAPERED TCPCF FILTERS

The transmission spectrums are measured for TCPCF filters before and after tapering as shown in Fig.6. At 1540-1550 nm and 1560-1580 nm, the spectrums after tapering have relatively high extinction ratio and clarity, which is consistent with our theoretical analysis. The FSR of the tapered TCPCF is smaller than that of TCPCF without tapering. This is because the mode coupling enhanced after tapering and the coupling coefficient increased. However, there is slight difference in terms of FSR in the highlighted region, which may because the inter-core coupling relies on phase matching between modes in the different cores and can therefore also be affected by possible phase shifts arising from slightly different propagation velocities of the modes in the different cores [37]. When the taper length exceeds 2000 μm, the extinction ratio and clarity of the spectrum decline, and the effective spectral width for exciting lasers decrease. Thus we only show the results with taper length smaller than 2000 μm.

III. EXPERIMENTAL SETUP AND RESULTS

A. EXPERIMENTAL SETUP

A ring laser is constructed by using the tapered TCPCF filter, as shown in Fig.7. The 980/1550 nm wavelength division multiplexer (WDM) is used to couple 980 nm pump source entering the erbium-doped fiber (EDF) and EDF serves as a gain medium. The used EDF with an absorption coefficient of 7 dB/m at 1531 nm has an optimized length of 10 m, which ensures the flatness and relatively high gain of its gain spectrum over 1565 nm. The isolator (ISO) is a single-mode isolator with a center wavelength of 1550nm (λc) and has low forward insertion loss (<0.4 dB, λc $\pm$ 20nm) and high reverse isolation (> 30dB, λc $\pm$ 15nm). It can prevent backscattered light and parasitic laser from transmitting back to the pump source. As a key device in the laser cavity, polarization controller (PC) can adjust the light polarization in the ring cavity. The lasing output is monitored by using an optical spectrum analyzer (OSA) with a resolution of 0.02 nm through the 10% port of the 90:10 coupler.

B. THE MODE SELECTION MECHANISM IN THE LASER OPERATION

TCPCF supports multiple fundamental super-modes, each of which has two orthogonal polarization states. Interference would appear between the super-modes with the same polarization state and results in the light power coupling among three cores [36]. This makes the gain spectrum of EDF into a comb-like spectrum with periodicity. By adjusting the states of the PC, the polarization state of incident light entering the TCPCF changes. Due to TCPCF filter is polarization dependent, its transmission functions are changed by incident light

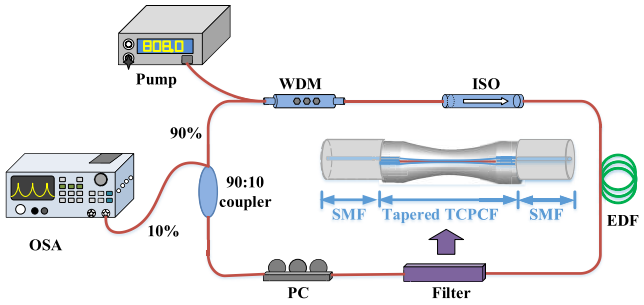

FIGURE 7. Schematic diagram of the ring cavity laser based on the tapered TCPCF filter.

with different polarization states [38]. Thus the polarization hole burning (PHB) effect can be achieved, which can greatly reduce homogeneous gain broadening of EDF and achieve multi-wavelength lasing outputs [39]. The peak wavelengths in the comb-like spectrum corresponding to high gain are easier to generate lasing outputs. However, only those peak wavelengths can form laser oscillation that the gain at the wavelength is greater than the loss it experiences [37].

C. MULTIPLE SETS OF TUNABLE DUAL-WAVELENGTH LASERS

When the first two coils of the PC are at an angle of 45° or 90°, rotating the third coil can achieve dual-wavelength lasing outputs with different intervals. However, continuously tunable dual-wavelength lasing outputs with a fixed wavelength interval could not achieve only through PC adjustment. To achieve continuous tunable lasing output, the position of PC is fixed and strain is applied to tapered TCPCF filter by putting the filter on the strain test device in Fig.8(a). One of the holders is fixed and the other holder is free to move to apply strain. The two ends of the filter are fixed into the two grooves by using super glue to prevent the fiber slide from the holders. The distance between two fixed points is 4 cm and the strain precise is 250 $\mu\varepsilon$.

Fig. 8(b-f) shows tunable dual-wavelength lasing outputs with a wavelength interval of 2-FSR. The output laser drifts towards the shorter wavelength direction continuously as the increase of strain. The tunable range for lasers based on un-tapered TCPCF (b) and tapered TCPCFs with the waist diameter of 136 μm (c), 130 μm (d), 126 μm (e), 121 μm (f) are 6 nm, 10.2 nm 10.76 nm, 14.36 nm and 10.22 nm, respectively. The maximum range of 14.36 nm is two times greater than that of the un-tapered TCPCF filter. This is mainly because the taper improves the comb characteristics of the transmission spectrum at L-band. The SMSR of the dual-wavelength lasers is further increased from 42 to 52 dB after tapering. This is attributed to the fact that the taper reduces the core size and the optical mode field area, which in turn leads to an increase in light intensity. Therefore, the extinction ratio of the transmission spectrum and the SMSR of the lasing output increase.

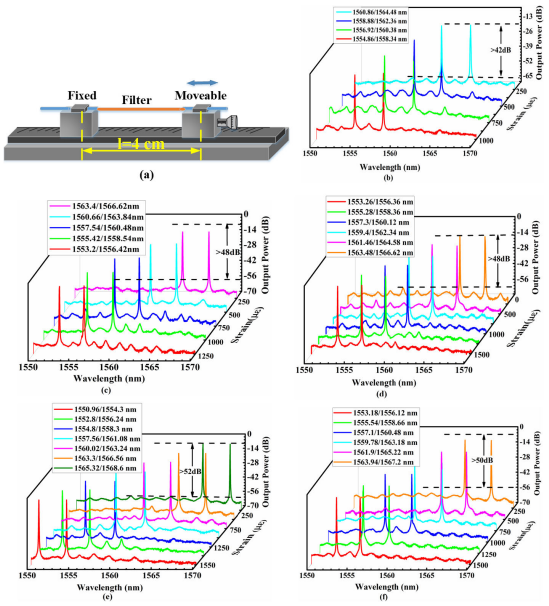

FIGURE 8. The strain tuning device (a). Tunable dual-wavelength lasing output of EDFL based on un-tapered TCPCF (b) and tapered TCPCFs with the waist diameter of 136 μm (c), 130 μm (d), 126 μm (e) and 121 μm (f) when the peak wavelength intervals is 2-FSR.

However, the tapered TCPCF filters can be used to suppress the mode competition but could not eliminate it. Gain competition still exists in the two peaks whose wavelength interval equals to the FSR in our experiment. During the tuning process, one of the two peaks will disappear or the third lasing line will appear. As the wavelength interval increases to 2-FSR, the stability of the output laser improves. This phenomenon has appeared in previous literature, which shows that wide wavelength intervals have relatively high stability [40], [41]. The relationship between the transmission spectrum and dual-wavelength lasing outputs during the tuning process is shown in Fig.9. Lasers are excited at

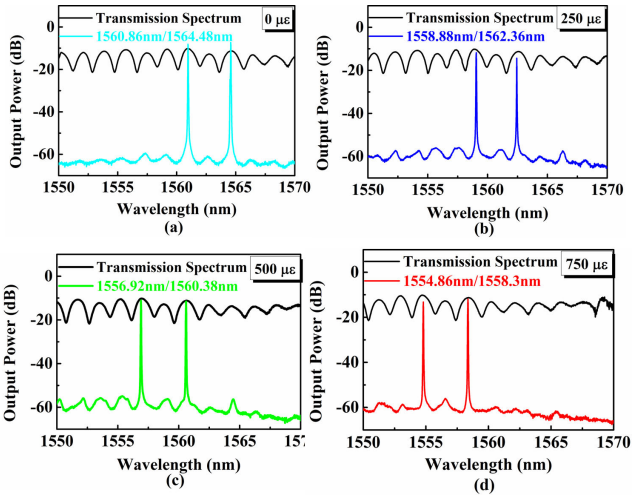

FIGURE 9. The relationship between transmission spectrum and dual-wavelength lasing output during the tuning process. The applied strain are 0 $\mu\varepsilon$ (a), 250 $\mu\varepsilon$ (b), 500 $\mu\varepsilon$ (c) and 750 $\mu\varepsilon$ (d), respectively.

the peak wavelength in the transmission spectrum of the filter. The tuning step and tuning range of output lasing are consistent with that of the transmission spectrum. Moreover, the dual-wavelength interval keeps unchanged during the tuning process.

Tapered TCPCFs with the same taper length but different taper modes achieve different tunable performance. A performance comparison for the wavelength interval of 3 to 4-FSR is summarized in Table 1. The tuning range and SMSR of tapers under non-scan mode are higher than that of frame-scan mode, which indicates the tapered TCPCF filter made by non-scan mode is more conducive to obtain good tuning characteristics. This is because the non-scan mode can achieve a thinner waist area under the same taper length. The mode coupling of the waist region is further enhanced, thereby increasing the gain of the output laser and widening the tunable range of the output laser. To get the optimal taper length under non-scan mode, a series of tapered TCPCFs with different taper lengths are fabricated with a length interval of 200 μm and tested as shown in Fig.10. As the taper length increases, the tunable range and the SMSR of lasing outputs increase first and then decrease. When the taper length increases to 1000 μm, this improvement reaches a peak. At this point, we get the best taper length under non-scan mode is 1000 μm and the corresponding waist diameter is 126 μm. This is consistent with our simulation results. This taper has the highest coupling coefficient and a high K value, so the transmission spectrum has high extinction ratio and wide comb spectrum. The output laser has a good consistency with the transmission spectrum, so the laser output performance with this taper is the best.

In addition to 2-FSR, the dual-wavelength laser output with a wavelength interval of 3-FSR and 4-FSR realized by this optimal taper also shows a wide tuning range of 12.68 nm and 10.96 nm as shown in Fig.11. However, the tunable range reduces with the increase of the dual-wavelength interval. This is because within the gain bandwidth of the EDF, the lasers can be generated within a certain wavelength range, which is determined by the filter. Within this wavelength range the larger the dual-wavelength interval, the smaller the tunable range.

TABLE 1. Tuning performance of dual-wavelength lasers with wavelength interval of 3-FSR and 4-FSR.

Taper Mode	Taper parameter		Tunable range (nm)		SMSR (dB)	
	Taper Length (μm)	Waist Diameter (μm)	3-FSR	4-FSR	3-FSR	4-FSR
Non-taper	0	144	6.34	4.02	>45	>42
Flame-scan	1000	136	8.14	5.98	>48	>47
Flame-scan	2000	130	9.56	7.36	>49	>48
Non-scan	**1000**	**126**	**12.68**	**10.96**	**>52**	**>52**
Non-scan	2000	121	10.28	9.02	>49	>50

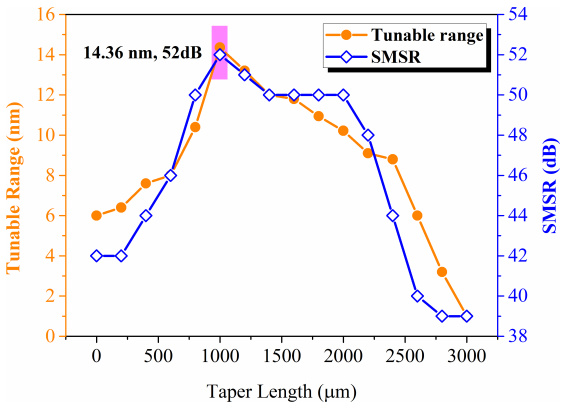

FIGURE 10. Under non-scan mode, the tunable performance of lasers with different taper lengths.

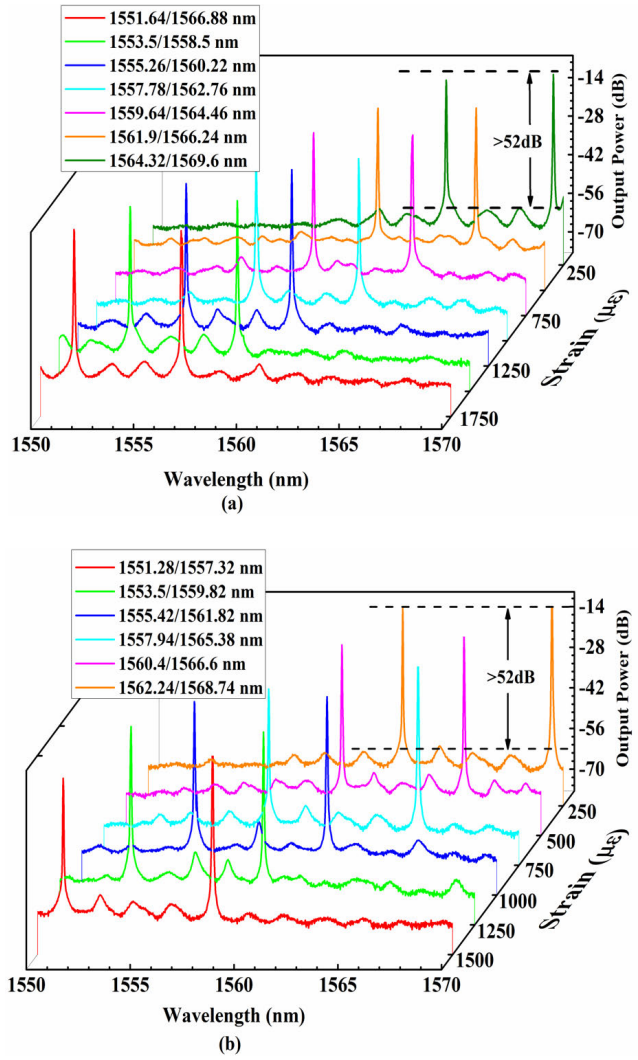

FIGURE 11. Tunable dual-wavelength lasers with the wavelength interval of 3-FSR (a) and 4-FSR (b).

D. STABILITY INVESTIGATION

The stability of the lasing output at room temperature is explored by scanning the lasing output every 20 minutes'

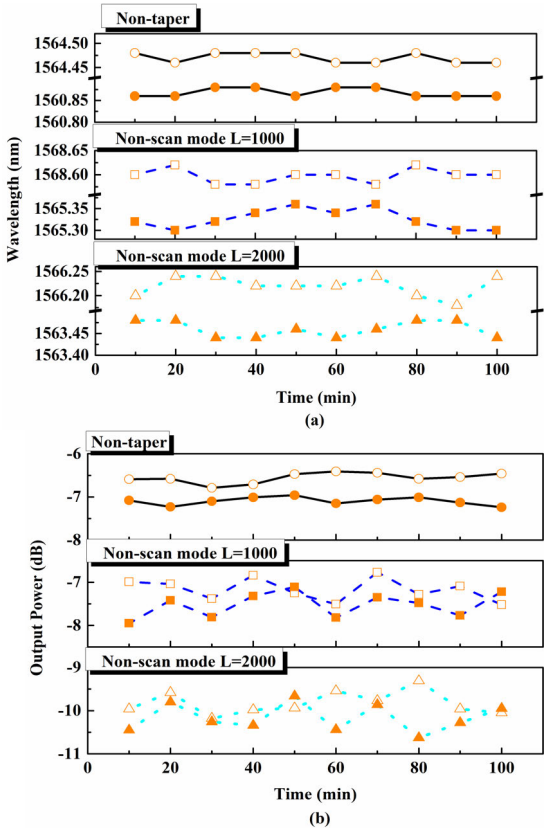

FIGURE 12. Peak wavelength shift (a) and peak power fluctuation (b) of dual-wavelength lasing output with a wavelength interval of 2-FSR.

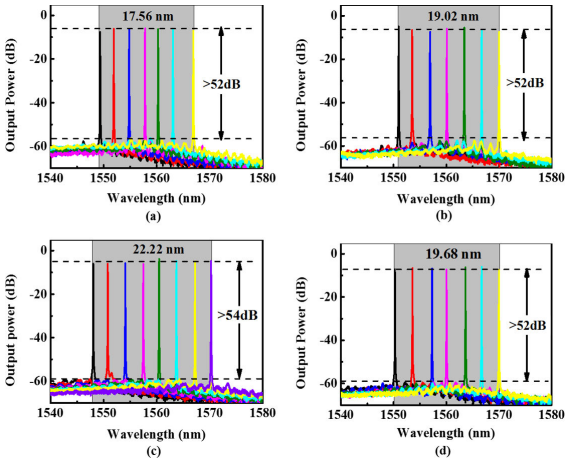

FIGURE 13. Tunable single-wavelength lasing output by using filters based on tapered TCPCF with the waist diameter of 136 μm (a), 130 μm (b), 126 μm (c), 121 μm (d).

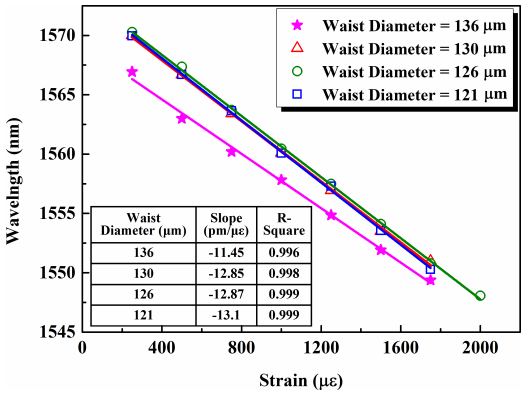

FIGURE 14. Linear fitting of single-wavelength laser with strain.

interval for 4 hours as shown in Fig.12. The peak wavelength and peak power of dual-wavelength lasing outputs with a wavelength interval of 2-FSR are monitored. The stability of the lasing output decrease as the taper waist diameter decrease. Although the taper reduces the stability of lasing output, there exists stable mode-coupling in the tapered TCPCF. The peak wavelength shift of each peak wavelength is less than 0.04nm. The peak power fluctuation at two peak wavelengths is less than 0.75 dB. This ensures the stability of the tapered TCPCF based lasers still meets the needs of practical applications. Besides, due to the homemade TCPCF is composed of pure silica, which has a low thermo-optic coefficient. Thus the laser we proposed has favorable temperature stability.

IV. DISCUSSION

A. TUNABLE SINGLE-WAVELENGTH LASING OUTPUT

When the first two coil planes of the PC are kept parallel and the third coil is rotated, single wavelength lasing output at different positions can be achieved. The tunable lasers are achieved using the strain device mentioned before as shown in Fig.13. The SMSR of all lasing output is higher than 52 dB. The tunable range for lasers based on tapered TCPCF with the waist diameter of 136 μm, 130 μm, 126 μm, 121 μm are 17.56 nm, 19.02 nm, 22.22 nm and19.68 nm, respectively. The tunable range is slightly higher than that of dual-wavelength. This is because at the edge of the gain bandwidth, the gain is relatively low. It is not enough to support the simultaneous output of lasers of two wavelengths because two lasers share gain at the same time.

A linear fit of the wavelength shift as a function of strain are shown in Fig.14. The slopes that represent the strain sensitives of four kinds of the tapered TCPCF sensors are -11.45 pm/$\mu\varepsilon$, -12.85 pm/$\mu\varepsilon$, -12.87 pm/$\mu\varepsilon$, and -13.1 pm/$\mu\varepsilon$, respectively. The maximum strain sensitivity of -13.1 pm/$\mu\varepsilon$ is higher than most of the fiber strain sensors reported in recent years. In addition, the output laser has high linearity with the applied strain, which indicates that this laser owns great application value in strain measurement.

B. TUNABLE TRIPLE-WAVELENGTH LASING OUTPUT

When the coils on both sides are at an angle of 180° and the center coil is rotated, triple-wavelength lasing output at different positions can be achieved. The tunable laser based on tapered TCPCF filter with a waist diameter of 126 μm can also generate tunable triple-wavelength lasing output with the wavelength interval of FSR to 3-FSR as shown in Fig.15. The

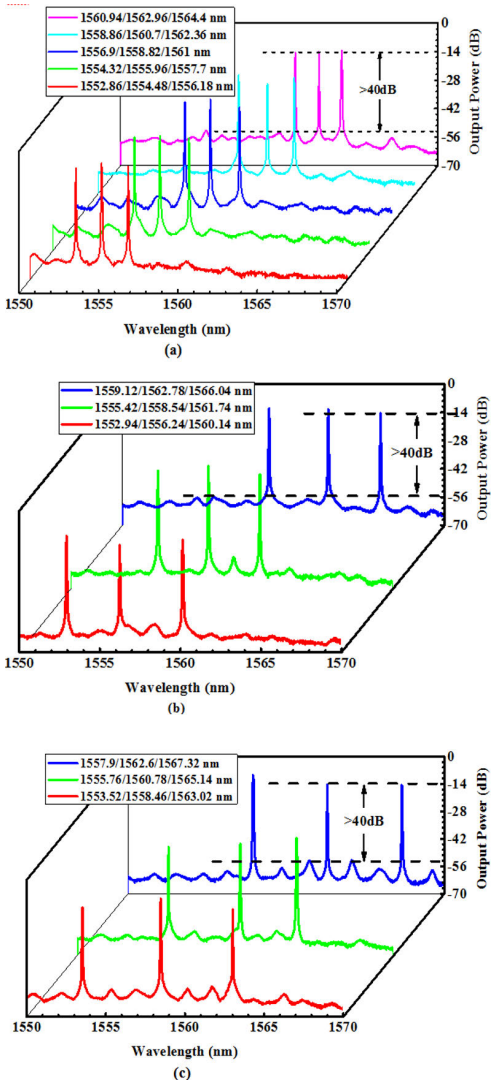

FIGURE 15. Tunable triple-wavelength lasers with peak wavelength interval of FSR (a), two times the FSR (b), three times the FSR (c).

tunable range are 8.08 nm, 6.18 nm and 4.38 nm, respectively. The SMSR of all lasing output is higher than 40 dB.

V. CONCLUSION

We proposed and experimentally demonstrated a multi-group dual-wavelength tunable EDFL by using the tapered TCPCF filters. The effect of the taper on the tunable characteristics of the laser is analyzed in theory and verified by making multiple sets of tapered TCPCF filters experimentally. Experimental results show that tapering 1000 μm long TCPCF by using non-scan mode can achieve the best tunable characteristics. Four kinds of tunable dual-wavelength lasers with different wavelength intervals can be obtained with the maximum tunable range of 14.36 nm. The lasing output shows good wavelength and peak power stability. In addition, tunable single-wavelength and triple-wavelength output lasing are also achieved. Three kinds of tunable triple-wavelength lasers are obtained with the maximum tunable range of 8.08 nm. Tunable single-wavelength lasing output exhibits high linearity with the applied strain, which has potential application value in the strain sensing area.

REFERENCES

[1] Y. Yao, X. Chen, Y. Dai, and S. Xie, "Dual-wavelength erbium-doped fiber laser with a simple linear cavity and its application in microwave generation," *IEEE Photon. Technol. Lett.*, vol. 18, no. 1, pp. 187–189, Jan. 1, 2006.

[2] A. A. Latiff, N. A. Kadir, E. I. Ismail, H. Shamsuddin, H. Ahmad, and S. W. Harun, "All-fiber dual-wavelength Q-switched and mode-locked EDFL by SMF-THDF-SMF structure as a saturable absorber," *Opt. Commun.*, vol. 389, pp. 29–34, Apr. 2017.

[3] B. Yin, S. Wu, M. Wang, W. Liu, H. Li, B. Wu, and Q. Wang, "High-sensitivity refractive index and temperature sensor based on cascaded dual-wavelength fiber laser and SNHNS interferometer," *Opt. Express*, vol. 27, no. 1, pp. 252–264, 2019.

[4] S. Yamashita and K. Hotate, "Multiwavelength erbium-doped fibre laser using intracavity etalon and cooled by liquid nitrogen," *Electron. Lett.*, vol. 32, no. 14, pp. 1298–1299, 1996.

[5] Z. Chen, S. Ma, and N. K. Dutta, "Multiwavelength fiber ring laser based on a semiconductor and fiber gain medium," *Opt. Express*, vol. 17, no. 3, pp. 1234–1239, 2009.

[6] L. Li, A. Schulzgen, V. L. Temyanko, C. Spiegelberg, D. T. Nguyen, X. Zhu, J. V. Moloney, J. Albert, and N. Peyghambarian, "Cladding-pumped distributed feedback phosphate glass fiber lasers," in *Proc. Conf. Lasers Electro-Opt.*, May 2008, pp. 1–2.

[7] P. Wang, L. Chen, X. Zhang, P. Gao, Z. Zhang, W. Jiang, W. Zhang, Y. Zhou, M. Liao, T. Suzuki, Y. Ohishi, and W. Gao, "Multi-wavelength fiber laser generated by brillouin-comb assisted four-wave mixing," *Opt. Commun.*, vol. 444, pp. 63–67, Aug. 2019.

[8] T. Liu, D. Jia, T. Yang, Z. Wang, and Y. Liu, "Stable L-band multi-wavelength SOA fiber laser based on polarization rotation," *Appl. Opt.*, vol. 56, no. 10, pp. 2787–2791, 2017.

[9] H. Ahmad, N. A. Hassan, S. N. Aidit, and Z. C. Tiu, "Generation of tunable multi-wavelength EDFL by using graphene thin film as nonlinear medium and stabilizer," *Opt. Laser Technol.*, vol. 81, pp. 67–69, Jul. 2016.

[10] Y. Li, J. Tian, M. Quan, and Y. Yao, "Tunable multiwavelength er-doped fiber laser with a two-stage lyot filter," *IEEE Photon. Technol. Lett.*, vol. 29, no. 3, pp. 287–290, Feb. 1, 2017.

[11] T. Feng, M. Jiang, D. Wei, L. Zhang, F. Yan, S. Wu, and X. S. Yao, "Four-wavelength-switchable SLM fiber laser with sub-kHz linewidth using superimposed high-birefringence FBG and dual-coupler ring based compound-cavity filter," *Opt. Express*, vol. 27, no. 25, pp. 36662–36679, 2019.

[12] H. Ahmad and A. A. Jasim, "Fabrication and characterization of 2 × 2 microfiber coupler for generating two output stable multiwavelength fiber lasers," *J. Lightw. Technol.*, vol. 35, no. 19, pp. 4227–4233, Oct. 1, 2017.

[13] M. Zhou, F. Ren, J. Li, D. Ge, Y. Zhang, Z. Chen, and Y. He, "Tunable multi-wavelength EDF laser based on Sagnac interferometer with weakly-coupled FMF delay line," in *Proc. Opt. Fiber Commun. Conf.* San Diego, CA, USA: Optical Society of America, Mar. 2018, Paper M2J.5.

[14] S. Wang, M. Lv, Y. Zhang, and X. Chen, "Wavelength-spacing-controllable multi-wavelength fiber laser based on a Lyot–Sagnac filter," *Appl. Opt.*, vol. 57, no. 30, pp. 8845–8850, 2018.

[15] J. Gutierrez-Gutierrez, R. Rojas-Laguna, J. M. Estudillo-Ayala, J. M. Sierra-Hernández, D. Jauregui-Vazquez, M. Vargas-Treviño, L. Tepech-Carrillo, and R. Grajales-Coutiño, "Switchable and multi-wavelength linear fiber laser based on Fabry–Pérot and Mach–Zehnder interferometers," *Opt. Commun.*, vol. 374, pp. 39–44, Sep. 2016.

[16] G. Yin, S. Lou, X. Wang, and B. Han, "Dual-wavelength erbium-doped fiber laser with tunable wavelength spacing using a twin core fiber-based filter," *J. Opt.*, vol. 16, no. 5, May 2014, Art. no. 055404.

[17] Y. Lian, G. Ren, B. Zhu, Y. Gao, W. Jian, W. Ren, and S. Jian, "Switchable multiwavelength fiber laser using erbium-doped twin-core fiber and nonlinear polarization rotation," *Laser Phys. Lett.*, vol. 14, no. 5, May 2017, Art. no. 055101.

[18] W. He, W. Zhang, L. Zhu, X. Lou, and M. Dong, "C-band switchable multi-wavelength erbium-doped fiber laser based on Mach–Zehnder interferometer employing seven-core fiber," *Opt. Fiber Technol.*, vol. 46, pp. 30–35, Dec. 2018.

[19] L. Zhang, Z. Tian, N.-K. Chen, H. Han, C.-N. Liu, K. T. V. Grattan, B. M. A. Rahman, H. Zhou, S.-K. Liaw, and C. Bai, "Room-temperature power-stabilized narrow-linewidth tunable erbium-doped fiber ring laser based on cascaded Mach–Zehnder interferometers with different free spectral range for strain sensing," *J. Lightw. Technol.*, vol. 38, no. 7, pp. 1966–1974, Apr. 1, 2020.

[20] L. Tong, R. R. Gattass, J. B. Ashcom, S. He, J. Lou, M. Shen, I. Maxwell, and E. Mazur, "Subwavelength-diameter silica wires for low-loss optical wave guiding," *Nature*, vol. 426, no. 6968, pp. 816–819, Dec. 2003.

[21] P. Wang, H. Zhao, X. Wang, G. Farrell, and G. Brambilla, "A review of multimode interference in tapered optical fibers and related applications," *Sensors*, vol. 18, no. 3, p. 858, Mar. 2018.

[22] A. A. Jasim and H. Ahmad, "A highly stable and switchable dual-wavelength laser using coupled microfiber Mach–Zehnder interferometer as an optical filter," *Opt. Laser Technol.*, vol. 97, pp. 12–19, Dec. 2017.

[23] Z.-R. Tong, H. Yang, and Y. Cao, "Tunable and switchable dual-wavelength erbium-doped fiber laser based on in-line tapered fiber filters," *Optoelectron. Lett.*, vol. 12, no. 4, pp. 264–267, Jul. 2016.

[24] Y. Zhou, S. Lou, Z. Tang, T. Zhao, and W. Zhang, "Tunable and switchable C-band and L-band multi-wavelength erbium-doped fiber laser employing a large-core fiber filter," *Opt. Laser Technol.*, vol. 111, pp. 262–270, Apr. 2019.

[25] K. Saitoh, Y. Sato, and M. Koshiba, "Polarization splitter in three-core photonic crystal fibers," *Opt. Express*, vol. 12, no. 17, pp. 3940–3946, 2004.

[26] K. Saitoh, N. J. Florous, M. Koshiba, and M. Skorobogatiy, "Design of narrow band-pass filters based on the resonant-tunneling phenomenon in multi-core photonic crystal fibers," *Opt. Express*, vol. 13, no. 25, pp. 10327–10335, 2005.

[27] D. M. Taylor, C. R. Bennett, T. J. Shepherd, L. F. Michaille, M. D. Nielsen, and H. R. Simonsen, "Demonstration of multi-core photonic crystal fibre in an optical interconnect," *Electron. Lett.*, vol. 42, no. 6, pp. 331–332, 2006.

[28] X. Sun, "Wavelength-selective coupling of dual-core photonic crystal fiber with a hybrid light-guiding mechanism," *Opt. Lett.*, vol. 32, no. 17, pp. 2484–2486, 2007.

[29] X.-H. Fang, M.-L. Hu, L.-L. Huang, L. Chai, N.-L. Dai, J.-Y. Li, A. Y. Tashchilina, A. M. Zheltikov, and C.-Y. Wang, "Multiwatt octave-spanning supercontinuum generation in multicore photonic-crystal fiber," *Opt. Lett.*, vol. 37, no. 12, pp. 2292–2294, 2012.

[30] X.-H. Fang, M.-L. Hu, B.-W. Liu, L. Chai, C.-Y. Wang, and A. M. Zheltikov, "Generation of 150 MW, 110 fs pulses by phase-locked amplification in multicore photonic crystal fiber," *Opt. Lett.*, vol. 35, no. 14, pp. 2326–2328, 2010.

[31] K. K. Qureshi, "Switchable dual-wavelength fiber ring laser featuring twin-core photonic crystal fiber-based filter," *Chin. Opt. Lett.*, vol. 12, no. 2, pp. 27–29, 2014.

[32] Z. Tang, S. Lou, and X. Wang, "Stable and widely tunable single-/dual-wavelength erbium-doped fiber laser by cascading a twin-core photonic crystal fiber based filter with Mach–Zehnder interferometer," *Opt. Laser Technol.*, vol. 109, pp. 249–255, Jan. 2019.

[33] M. Alouini, M. Brunel, F. Bretenaker, M. Vallet, and A. Le Floch, "Dual tunable wavelength Er,Yb: Glass laser for terahertz beat frequency generation," *IEEE Photon. Technol. Lett.*, vol. 10, no. 11, pp. 1554–1556, Nov. 1998.

[34] W. J. Wadsworth, A. Witkowska, S. G. Leon-Saval, and T. A. Birks, "Hole inflation and tapering of stock photonic crystal fibres," *Opt. Express*, vol. 13, no. 17, pp. 6541–6549, 2005.

[35] A. W. Snyder, "Coupled-mode theory for optical fibers," *J. Opt. Soc. Amer.*, vol. 62, no. 11, pp. 1267–1277, 1972.

[36] Y. Chunxia, D. Hui, D. Wei, and X. Chaowei, "Weakly-coupled multicore optical fiber taper-based high-temperature sensor," *Sens. Actuators A, Phys.*, vol. 280, pp. 139–144, Sep. 2018.

[37] Y. Yan and J. Toulouse, "Polarization dependence of the inter-core coupling in triple-core photonic crystal fibers," *J. Opt. Soc. Amer. B, Opt. Phys.*, vol. 26, no. 4, pp. 762–767, 2009.

[38] Y. Huo and P. K. Cheo, "Analysis of transverse mode competition and selection in multicore fiber lasers," *J. Opt. Soc. Amer. B, Opt. Phys.*, vol. 22, no. 11, pp. 2345–2349, 2005.

[39] W. He, G. Zhong, L. Zhu, M. Dong, and G. Chen, "Wavelength-switchable erbium-doped fiber laser based on femtosecond FBG inscribed on fiber core and cladding through the coating," *Laser Phys. Lett.*, vol. 16, no. 5, May 2019, Art. no. 055104.

[40] S. Li, K. S. Chiang, and W. A. Gambling, "Fast accurate wavelength switching of an erbium-doped fiber laser with a Fabry–Pérot semiconductor filter and fiber Bragg gratings," *Appl. Phys. Lett.*, vol. 77, no. 26, pp. 4268–4270, Dec. 2000.

[41] K. Yang, J. He, C. Liao, Y. Wang, S. Liu, K. Guo, J. Zhou, Z. Li, Z. Tan, and Y. Wang, "Femtosecond laser inscription of fiber Bragg grating in twin-core few-mode fiber for directional bend sensing," *J. Lightw. Technol.*, vol. 35, no. 21, pp. 4670–4676, Nov. 1, 2017.

ZIJUAN TANG was born in Shanxi, China, in 1993. She received the bachelor's degree from the School of Electronic and Information Engineering, Beijing Jiaotong University, in 2016, where she is currently pursuing the Ph.D. degree in communication and information system. Her research interests include fiber sensors and lasers-based on special fibers.

ZHENGGANG LIAN received the bachelor's and Ph.D. degrees in electronic engineering from the University of Nottingham, in 2006 and 2010, respectively. He worked with the Optoelectronics Research Centre, University of Southampton. Since 2014, he has been working with Wuhan Yangtze Optical Electronics Company Ltd., where he oversees the Research and Development Department. He joined the Huazhong University of Science and Technology, as a part-time Professor, in 2016. He has generated more than 60 publications and 16 patents. His research interests include design and fabrication of specialty optical fibers, targeting application includes optoelectronic sensing, IR transmission, and high-power fiber lasers.

TREVOR M. BENSON (Senior Member, IEEE) received the degree (Hons.) in physics and the Ph.D. degree in electronic and electrical engineering from The University of Sheffield, Sheffield, U.K., in 1979 and 1982, respectively, and the D.Sc. degree from the University of Nottingham, Nottingham, U.K., in 2005.

After spending more than six years as a Lecturer with the University College Cardiff, he joined the University of Nottingham, in 1989. He became a Chair in optoelectronics in 1996, having previously been a Senior Lecturer, in 1989, and a Reader, in 1994. Since October 2011, he has been the Director of the George Green Institute for Electromagnetics Research, University of Nottingham. His research interests include experimental and numerical studies of electromagnetic fields and waves with particular emphasis on the theory, modeling and simulation of optical waveguides, lasers and amplifiers, nano-scale photonic circuits, and electromagnetic compatibility.

Dr. Benson is a fellow of the Institute of Engineering Technology and the Institute of Physics. He became a fellow of the Royal Academy of Engineering for his achievement in the development of versatile design software used to analyze propagation in optoelectronic waveguides and photonic integrated circuits, in 2005. He was a recipient of the Clark Prize in experimental physics.

XIN WANG received the Ph.D. degree from Beijing Jiaotong University, Beijing, China, in 2016. She is currently an Associate Professor with the School of Electronic and Information Engineering, Beijing Jiaotong University. She has authored or coauthored more than 20 articles on international journals, including the IEEE JOURNAL OF SELECTED TOPICS IN QUANTUM ELECTRONICS, the IEEE PHOTONICS JOURNAL, *Applied Optics*, and so on. Her research interests include micro-structured fiber, fiber property, and fabrication.

WAN ZHANG received the B.S. and M.S. degrees from Yanshan University, Qinhuangdao, China, in 2012 and 2015, respectively. She is currently pursuing the Ph.D. degree with Beijing Jiaotong University, Beijing, China. Her research interests include micro-structured fiber, hollow core anti-resonant fiber, fiber sensor, surface plasmon resonance, and communication and information systems.

SHIBO YAN was born in Liaoning, China, in 1992. He received the B.S. degree from Beijing Jiaotong University, Beijing, China, in 2015, where he is currently pursuing the Ph.D. degree in communication and information engineering. His current research interests include hollow core anti-resonant fiber, Terahertz waveguide, and so on.

SHUQIN LOU (Member, IEEE) received the Ph.D. degree from Beijing Jiaotong University, Beijing, China, in 2005. She is currently a Professor with the School of Electronic and Information Engineering, Beijing Jiaotong University. She has authored or coauthored more than 200 articles on international journals, including *Optics Express*, the IEEE PHOTONICS TECHNOLOGY LETTERS, the IEEE/OSA JOURNAL OF LIGHTWAVE TECHNOLOGY, and so on. Her current research interests include micro-structured fiber, fiber components, fiber laser, and fiber sensor.